HHS Public Access

Author manuscript

Magn Reson Med. Author manuscript; available in PMC 2025 October 01.

Published in final edited form as:

Magn Reson Med. 2024 October ; 92(4): 1348–1362. doi:10.1002/mrm.30158.

GABA-edited MEGA-PRESS at 3T: Does a measured MM background improve linear combination modeling?

Christopher W. Davies-Jenkins[1,2], **Helge J. Zöllner**[1,2], **Dunja Simicic**[1,2], **Steve C. N. Hui**[3,4,5], **Yulu Song**[1,2], **Kathleen E. Hupfeld**[1,2], **James J. Prisciandaro**[6], **Richard A.E. Edden**[1,2], **Georg Oeltzschner**[1,2,*]

[1]The Russell H. Morgan Department of Radiology and Radiological Science, Johns Hopkins University School of Medicine, Baltimore, MD, USA

[2]F.M. Kirby Research Center for Functional Brain Imaging, Kennedy Krieger Institute, Baltimore, MD, USA

[3]Developing Brain Institute, Children's National Hospital, Washington, DC, USA

[4]Department of Radiology, The George Washington School of Medicine and Health Sciences, Washington D.C., USA

[5]Department of Pediatrics, The George Washington School of Medicine and Health Sciences, Washington D.C., USA

[6]Department of Psychiatry and Behavioral Sciences, Addiction Sciences Division, Center for Biomedical Imaging, Medical University of South Carolina, Charleston, SC, USA

Abstract

Purpose—The J-difference edited GABA signal is contaminated by other co-edited signals—the largest of which originates from co-edited macromolecules (MMs)—and is consequently often reported as "GABA+". MM signals are broader and less well-characterized than the metabolites, and so are commonly approximated using a Gaussian model parameterization. Experimentally measured MM signals are a consensus-recommended alternative to parameterized modeling; however, they are relatively under-studied in the context of edited MRS.

Methods—To address this limitation in the literature, we have acquired GABA-edited MEGA-PRESS data with pre-inversion to null metabolite signals in 13 healthy controls. An experimental MM basis function was derived from the mean across subjects. We further derived a new parameterization of the MM signals from the experimental data, using multiple Gaussians to accurately represent their observed asymmetry. The previous single-Gaussian parameterization,

*Corresponding author: Georg Oeltzschner, Ph.D., Division of MR Research, Russell H. Morgan Department of Radiology and Radiological Science, The Johns Hopkins University School of Medicine, 600 N Wolfe St, Park 367H, Baltimore, MD 21287, goeltzs1@jhmi.edu.

Ethical approval and consent

The study protocol and consent forms were approved by the Institutional Review Board of the Johns Hopkins University School of Medicine. Written informed consent was obtained from all participants prior to their enrollment in the study.

Consent for publication

All authors consent to the publication of this study.

mean experimental MM spectrum and new multi-Gaussian parameterization were compared in a three-way analysis of a public MEGA-PRESS dataset of 61 healthy participants.

Results—Both the experimental MMs and the multi-Gaussian parameterization exhibited reduced fit residuals compared to the single-Gaussian approach ($p = 0.034$ & $p = 0.031$, respectively), suggesting they better represent the underlying data than the single-Gaussian parameterization. Furthermore, both experimentally derived models estimated larger MM fractional contribution to the GABA+ signal for the experimental MMs (58%) and multi-Gaussian parameterization (58%), compared to the single-Gaussian approach (50%).

Conclusions—Our results indicate that single-Gaussian parameterization of edited MM signals is insufficient and that both experimentally derived GABA+ spectra and their parameterized replicas improve the modeling of GABA+ spectra.

Keywords

Macromolecules; MEGA-PRESS; metabolite-nulled; GABA; GABA+

1. Introduction

γ-aminobutyric acid (GABA) is the primary inhibitory neurotransmitter in the human brain, playing a crucial role in regulating neural activity. Magnetic resonance spectroscopy (MRS) is a technique that allows non-invasive in-vivo detection of GABA and several other endogenous brain neurometabolites. However, at clinically relevant field strengths, the GABA signal strongly overlaps with the resonances of more abundant compounds like creatine (Cr). J-difference editing techniques—such as MEGA-PRESS—feature frequency-selective editing pulses to refocus the coupling evolution of the 3-ppm GABA signal in one half of the experiment ("edit-ON"), while allowing the coupling to evolve freely in the other half ("edit-OFF"). Subtraction of the two sub-spectra retains only those signals affected by the editing pulse and removes overlapping signals that are identical in both halves[1–5].

Although spectral editing removes the strong Cr signal, accurate quantification of the GABA signal is still not straightforward. The limited frequency selectivity of editing pulses causes signals from other J-coupled molecules with similar spin systems to "co-edit". The edited 3-ppm GABA signal is therefore contaminated by contributions from mobile macromolecules (MM) and homocarnosine (HCar)[6]. The co-edited 3-ppm MM contribution is attributed to lysine-containing groups with coupling partners at ~1.7 ppm. The elegant symmetric MM suppression scheme[6,7] features an additional editing pulse in the "edit-OFF" sub-experiment, placed at 1.5 ppm so that the MM are equally co-edited in both halves and subtracted out. This experiment requires near-perfect symmetry of the editing pulses around the MM coupling partner, making it an order of magnitude more susceptible to pulse offsets caused by incorrect calibration, subject motion, or thermal scanner drift[8–10]. Real-time transmitter frequency updating methods stabilize the acquisition but are not available for all platforms and implementations. Conventional (non-symmetric) editing remains popular despite the 'impure' GABA measurement, and it is common practice to report "GABA+"—an acknowledgment that the quantified signal amplitude contains contributions from signals other than GABA[1].

Accurate modeling of the GABA+ signal is complicated by the lack of detailed knowledge about the shape of the co-edited MM signal. The default LCModel 'MEGA-PRESS' settings lack an MM model altogether, leaving a substantial part of the observed signal unmodeled. Gannet and Tarquin model the composite GABA+ peak with one and two Gaussians, respectively, but without a dedicated GABA-only signal model[11]. We have previously investigated strategies for linear-combination modeling of GABA-edited difference spectra, representing the co-edited MM as parametrized single-Gaussian signals in separate basis functions[12]. While the inclusion of a dedicated co-edited MM model reduced fit residuals and coefficients of variation across a large cohort of healthy participants, it is unclear whether the simplified parameterization as a single Gaussian describes the co-edited MM signal adequately.

The use of experimentally acquired MM basis functions has been recommended by recent MRS expert consensus and is relatively well-investigated in short-TE conventional (non-edited) spectra[13–21], but investigations of GABA-edited MMs are less common. Previous studies have attempted to directly subtract subject-level edited MMs from the data[22–24], compared integral areas of GABA and overlapping MMs[3], and explored LCModel parameterizations, indirectly incorporating MMs[25]. Additionally, we found two application studies that actually incorporated experimentally acquired edited MMs in the basis set[26,27], but we found no systematic exploration of the effect this has on GABA-edited difference spectra.

To address this gap and better characterize the MM background signal in GABA-edited difference spectra, we acquired inversion-recovery-prepared MEGA-PRESS data. We processed the metabolite-nulled spectra to generate an averaged edited MM spectrum that we then converted into a noise-free edited MM basis function. Furthermore, we refined our previously published best-practice single-Gaussian parameterization of the co-edited MM signals[12]: we derived a composite, multiple-Gaussian model from the experimental MM profile which improved the representation of the asymmetry of the co-edited MM signals[12,16]. Finally, we compared these two new MM modeling methods (experimental and multi-Gaussian parametrized MM basis functions) to our previously published best practice parameterization, using a large publicly available MEGA-PRESS dataset ("Big GABA"[28]).

2. Methods

2.1. Experimental edited MMs

2.1.1. ERecruitment—Experimental MM profiles were acquired in 13 healthy volunteers (mean age = 31 ± 5 years, 5 female). All participants provided written and informed consent, as approved by the local Institutional Review Board.

2.1.2. MM acquisition protocol—MR data were acquired on a 3T Philips Ingenia MR system (Philips Healthcare, Best, The Netherlands) using a 32-channel receive array head coil. The protocol included a T_1-weighted structural image (MPRAGE) for voxel placement. Metabolite-nulled GABA-edited MEGA-PRESS spectra (TR/TE = 2000/68 ms; 14-ms sinc-Gaussian editing pulses applied at 1.9/7.5 ppm; 256 transients; including interleaved water-unsuppressed reference scans[8]) matching the Big GABA protocol were acquired from

a 27-ml cubic voxel placed in the posterior cingulate cortex (PCC). Metabolite signals were nulled with a pre-inversion module, exploiting differences in T_1 relaxation times between MMs and metabolites[29–32]. Following previous work which identified the null point of Cr to be 500–650 ms[21], we opted for a denser sampling of inversion time (TI) to accurately determine the ideal value. As such, in 2 participants, the TI was iterated between 500–650 ms at 30-ms intervals. An optimal TI of 650 ms was found to minimize residual metabolite signals, as shown in Figure 1A (2nd subject shown in Supplementary Figure S1). This choice of TI was further supported by the reported T_1 of GABA[33] at 3T, which suggests that GABA should be almost perfectly nulled at 650 ms (Supplementary Figure S2). GABA-edited MM spectra were therefore subsequently acquired at TI = 650 ms in the remaining cohort for a total of 13 volunteers (MRSinMRS[34] summary may be found in Supplementary Table S1). In the same session, a second MEGA-PRESS acquisition was made with identical settings but without pre-inversion which, in this study, was used to estimate shim quality.

2.1.3. MM processing—All data were processed in Osprey[35] (v2.5.0, Matlab 2022a), an open-source LCM toolbox that conforms to expert consensus recommendations[36,37]. Raw data were coil-combined and eddy-current corrected using the water-unsuppressed reference scan[38]. Individual transients were aligned using robust spectral registration[39]. Lipid filtering of the MM spectra was performed using an L2-regularized method[40]. An artificial lipid basis matrix, L, was constructed using the following time-domain signal model:

$$S\left(t\right) = \sum_{k=1}^{m} A_k \, e^{-d_k|t - T/2|} e^{-i(2\pi f_k t \, + \, \Phi_k)}$$

where m is the total number of lipid signal components, A_k is the kth amplitude, d_k is the kth damping factor, T is the length of the time-domain signal, f_k is the kth precessional frequency, and Φ_k is the kth signal phase. For this study, we adapted the parameters chosen by Lin et al, reducing the number of lipid components and narrowing the range of frequencies and damping factors. This reduced computation time and—upon testing—satisfactorily removed the lipid signals encountered in our single-voxel in-vivo data. We included 128 lipid components with f_k in the range 1.0–1.6 PPM, d_k = 10–30 Hz, and Φ_k = 0 ± 1.8 rad. The inverse of the basis matrix, L^{-1}, is defined as:

$$L^{-1} = \left(\mathbb{1} + \beta\left(L \bullet L^{\dagger}\right)\right)^{-1}$$

where $\mathbb{1}$ is the identity matrix, β is a regularization parameter, and $L^{\dagger}$ is the conjugate transpose of L. The lipid filtered spectrum, S', is then calculated simply: $S' = L^{-1} \bullet S$, where S is the original lipid contaminated data. Residual metabolite signals remain in the nulled spectra due to inherent differences in T_1 values. Residual metabolite contributions to the MM spectra were removed from the individual sub-spectra using a linear-combination modeling approach. The edit-ON and edit-OFF MM spectra were modeled separately with a highly flexible cubic spline baseline and basis functions for N-acetylaspartate (NAA), glutamate (Glu), and water. In both sub-spectra, the identified residual contributions from

these signals were subtracted from the subject-level MMs, prior to the creation of the difference spectrum. Contributions from total creatine (tCr) and choline (tCho) compounds were satisfactorily removed by subtraction during the creation of the MM difference spectra. 'Cleaned' individual MM spectra were frequency-aligned to the 0.9 ppm MM resonance ($MM_{0.94}$). Individual MM spectra that retained significant lipid contributions or other artifacts were manually identified and removed from the analysis. All remaining individual MM spectra were averaged, and the resulting mean MM spectrum was fit with a flexible cubic B-spline (knot spacing = 0.03 ppm) to generate a smooth noise-free basis function that could be used as a basis function during LCM analysis. Figure 1B shows the MM spectra at various stages of MM cleanup, as well as the final basis function. Several resonances are apparent, resulting from direct and indirect effects of the 1.9 ppm editing pulse.

2.2. Analysis using Big GABA cohort

To examine the effect of including the newly derived experimentally acquired edited MMs, we included the edited MM basis function in the analysis of 61 MEGA-PRESS spectra from a recent multi-site study ("Big GABA"[28]). This subset was collected using Philips 3T scanners and identical acquisition parameters. We compared the experimental MM modeling approach to our previously published[12] parameterization of the co-edited 3-ppm MM signal as a single Gaussian, as well as to a new, refined parameterization informed by the experimental MM profiles.

Big GABA data were processed in Osprey as described previously[12]. In addition to the relevant MM parameterization, the basis sets included simulated profiles for ascorbate, Asc; aspartate, Asp; Cr; gamma-aminobutyric acid, GABA; glycerophosphocholine, GPC; glutathione, GSH; glutamine, Gln; glutamate, Glu; myo-inositol, mI; lactate, Lac; N-acetylaspartate, NAA; N-acetylaspartylglutamate, NAAG; phosphocholine, PCh; phosphocreatine, PCr; phosphorylethanolamine, PE; scyllo-inositol, sI; taurine, Tau. Metabolite and MM amplitudes were quantified as ratios to tCr.

For all three MM modeling approaches, the fit range was fixed at 0.5–4.0 ppm, the 1.2–1.9 ppm frequency range was excluded from the modeling of the difference spectrum, and a spline baseline was included with a knot spacing of 0.55 ppm[12]. The three MM fitting approaches each included a single additional basis function to represent the MMs, as defined in the following sections.

2.2.1. Parameterized MM: single-Gaussian—Our previous work investigated a range of modeling strategies for MMs in GABA-edited MRS[12]. The best-practice strategy we arrived at uses a single composite MM basis function which included individual Gaussian peaks at around 0.9 ppm (chemical shift, 0.915 ppm; FWHM, 11 Hz) and 3 ppm (chemical shift, 3.00 ppm; FWHM, 14 Hz) with a fixed amplitude ratio of 3/2. The basis function was scaled so that the area under the 3-ppm resonance ($MM_{3.0}$) corresponded to a CH_2 group[41]. During spectral modeling, the MM basis function—like the other metabolites—was allowed an MM-specific Lorentzian line broadening term but shared a Gaussian linebroadening term with the metabolite basis functions.

2.2.2. Experimental MM—The mean experimental noise-free MM spectrum—as derived in 2.1.3—was included in spectral modeling as a single basis function. Scaling of the experimental MM basis function was performed by normalizing the integral of $MM_{3.0}$ to a CH_2 group, following the subtraction of a linear baseline. As the experimental MM basis function was derived from in-vivo data, it had already experienced in-vivo Lorentzian and Gaussian linebroadening (in contrast to the simulated basis functions of the metabolites). Consequently, separate Gaussian and Lorentzian line-broadening terms were allowed for the MM, but initialized to zero.

2.2.3. Parameterized MM: new multiple-Gaussian approach—Upon investigation of the experimentally acquired MM spectrum, we noted substantial asymmetries of the major MM resonances that would be insufficiently characterized by single-Gaussian models. Furthermore, we noticed the presence of an additional co-edited MM resonance around 2 ppm ($MM_{2.05}$) that had not been considered in our previous parameterization. This motivated us to define a new, more adequate parameterization of the edited MMs. To this end, the three main resonances ($MM_{0.94}$, $MM_{2.05}$, $MM_{3.0}$) of the experimentally acquired MM spectrum were fit using multiple Gaussians using AMARES[42], as previously described[43]. Soft constraints were used to delineate the frequency ranges that fully encompassed each of the three main MM resonances. We attempted to minimize the number of Gaussian functions that contributed to each resonance, iteratively adding Gaussians until the residual was satisfactorily flat. The $MM_{0.94}$ resonance was modeled using 2 Gaussians with frequency soft constraints (0.74–0.98 ppm) and the phase fixed to 0. The asymmetric resonances at 2.0 and 3.0 ppm were modeled using 3 Gaussians, with frequency soft constraints of 1.80–2.15 ppm and 2.85–3.10 ppm, and the phase fixed at 180 and 0, respectively. The linewidth soft constraints were set in the range of 0–30 Hz for all Gaussian peaks, while the amplitude was left as a free parameter. The resulting parameters of the multiple-Gaussian fit are shown in Table 1. The experimental MM, single-Gaussian, and multiple-Gaussian basis functions that formed the basis of a three-way comparative analysis are shown in Figure 2.

Similar to the previous strategies, the integral over the $MM_{3.0}$ basis function was scaled to a CH_2 group prior to fitting. Since this parameterization was derived from in-vivo data, separate Gaussian and Lorentzian line-broadening terms were again allowed for the MM and metabolites during LCM.

All three MM handling methods are implemented in Osprey and can be specified in the job file using the appropriate option for “opt.fit.CoMM3” (https://github.com/schorschinho/osprey/tree/develop).

2.3. Statistical analysis

We compared metabolite estimates from the GABA-edited difference spectrum fit between the different MM analysis approaches with paired t-tests. Specifically, we considered the estimates for GABA, MM, and the composite GABA+ (GABA+MM) amplitudes, normalized to tCr from the edit-OFF spectrum (which was identical for all three approaches). Furthermore, we investigated the quality of the three modeling approaches

with two metrics, the amplitude and standard deviation of the fit residual across the fit range. Here, the residual amplitude was defined as the difference between the maximum and minimum of the fit residual. Both metrics were normalized to the height of the NAA peak from the edit-OFF spectrum. This residual analysis was conducted for two frequency ranges: (i) the full range (0.5–4.0 ppm, excluding the 1.2–1.9 ppm gap as described above) and (ii) specifically the range covered by the GABA+ signal (2.93–3.12 ppm). Statistical analyses were conducted in RStudio (version 4.2.0)[44].

3. Results

3.1. Experimental MMs

An example inversion recovery series is shown in Figure 1A, which depicts the difference spectra and the edit-OFF spectra. Metabolite signal contributions—as evidenced by the singlet at 2 ppm, for example—were found to be minimized around TI = 650 ms. To create a mean MM basis function that was free from contamination in the $MM_{0.94}$ signal region, we excluded MM spectra with visible lipid signals quite aggressively. 7 MM spectra were excluded; the remaining 6 spectra were then used to generate the MM basis function and were generally of high quality. The mean full-width at half maximum (FWHM) of the 2 ppm NAA singlet was 5.7 ± 0.8 Hz, as estimated from the edit-OFF spectrum acquired without pre-inversion. The $MM_{0.94}$ SNR was 15.2 ± 6.2, as calculated using the amplitude of the $MM_{0.94}$ peak in the MM difference spectrum. Both SNR and FWHM fulfilled expert consensus recommended quality requirements[36].

3.2. Analysis of the Big GABA Cohort

All 61 MEGA-PRESS spectra were successfully quantified by the three MM modeling strategies. Figure 3 shows (from top to bottom) the fit residuals, baseline, GABA fit, co-edited MM fit, co-edited Glu + Gln + GSH fit, and the overall LCM fit of the Big GABA cohort for the three MM modeling approaches. We noted a reduced mean fit residual around the GABA+ peak (shaded region) for the experimental MMs—and to a lesser extent the multiple-Gaussian MM—compared to the single-Gaussian approach, which features a prominent inverted GABA pseudo triplet. This suggested that the two new approaches improve the characterization of the observed signal and that the single-Gaussian model is overfitting GABA to compensate for inaccuracy in the MM model. Furthermore, including the co-edited $MM_{2.05}$ resonance in the multiple-Gaussian and experimental MM fits led to a flatter baseline in the respective region compared to the single-Gaussian parameterization, where the $MM_{2.05}$ is not explicitly handled at the basis-function level and therefore has to be absorbed by the spline baseline. Notably, the signal contribution from MM to the GABA+ peak is larger for the experimental MMs and multiple-Gaussian parameterization, than for the single-Gaussian parametrization. Consequently, the GABA contribution is lower.

Figure 4 summarizes the quantitative analysis of tCr-referenced GABA, MMs, and GABA+ estimates obtained with the three approaches. As observed in Figure 3, GABA/tCr was significantly lower for the experimental MM (0.015 ± 0.049; mean reduction 21%, $p < 0.001$) than for the single Gaussian (0.19 ± 0.05). The multi-Gaussian approach estimated GABA/tCr (0.15 ± 0.043) in line with the experimental MM—albeit with a lower

standard deviation—and lower than the single Gaussian (mean reduction 21%, $p < 0.001$). Consequently, higher MM/tCr ratios were found for the experimental MM (0.21 ± 0.039; mean increase 11%, $p = 0.007$) than the single-Gaussian (0.19 ± 0.03) approach, with the multi-Gaussian approach again aligning with the experimental MMs, reporting significantly higher MM than the single Gaussian (0.21 ± 0.038; mean increase 10%, $p = 0.009$).

The composite estimate, GABA+/tCr, did not significantly differ between any method. The experimental MM (0.36 ± 0.067) and single-Gaussian parameterization (0.38 ± 0.069) came the closest to significance (mean difference = 5%, $p = 0.10$).

Figure 5 shows quantitative model quality metrics, i.e., the amplitudes and standard deviations of the fit residual (first for the full fit range, then for the GABA+ signal range). Statistical analysis confirmed that overall fit quality was significantly improved by the experimental MMs and multiple-Gaussian parameterization compared to the previous, single-Gaussian approach. The full-range residual amplitude was 0.092 ± 0.028 for the single-Gaussian approach, and 0.081 ± 0.026 for the experimental MM (mean reduction 12%, $p = 0.034$) and the multiple-Gaussian MMs 0.081 ± 0.026 (mean reduction 12%, $p = 0.031$). While a similar pattern is qualitatively observed for the GABA-specific residual amplitudes (Figure 5), the differences were not statistically significant: Single-Gaussian MMs (0.026 ± 0.066), experimental MMs (0.025 ± 0.007), and multiple-Gaussian MMs (0.025 ± 0.008).

A similar pattern was observed for the standard deviation of the fit residuals. Compared to the single Gaussian (0.011 ± 0.003), the standard deviation of the full-range residual was significantly lower for the experimental MMs (0.010 ± 0.0025, mean reduction 9%, $p = 0.047$) and the multiple-Gaussian (0.010 ± 0.0025, mean reduction 9%, $p = 0.008$). Supplementary Table S2 contains the full descriptive statistics of the GABA, MM, GABA+, and model performance metrics, while Supplementary Table S3 contains the p-value results of the paired t-tests of these measures.

4. Discussion

Adequate modeling of in-vivo MR spectra is important for accurate estimation of metabolite concentrations, the primary outcome measures of MRS experiments. The diversity and complexity of contemporary linear-combination modeling algorithms has given rise to a surprising analytic variability of metabolite level estimates, with great influence wielded by fit settings and optimization hyperparameters[11,12,45–47]. One particularly impactful aspect of modeling is the treatment of broad resonances from MMs, i.e., peptides and proteins[13]. Spin systems of low-weight metabolites have been measured with great precision[48], allowing their spectra to be predicted with density-matrix simulations[49,50]. In contrast, the origin and characteristics of MM signals are less well understood, and an accurate model to describe them is still lacking. Their contributions to in-vivo spectra are therefore estimated based on simplified parametrizations or experimental data. These practices are relatively well investigated in short-TE spectra[13–20], but less so for J-difference edited spectra, although the relative contribution of MM to the signal of interest is even greater, for example, in GABA-edited MEGA-PRESS. Although expert consensus recommends using

experimentally acquired MM profiles in LCM[13], this practice has not been systematically investigated in the context of *J*-difference editing.

In this study, we acquired MEGA-PRESS spectra with a pre-inversion pulse to characterize MM contributions to GABA-edited difference spectra. We generated a cohort-mean GABA-edited MM basis function that was then used to fit a large GABA-edited MEGA-PRESS dataset. We then compared metabolite estimates and fit quality metrics for three MM modeling approaches: (1) the new 'experimental MM' approach; (2) our previously recommended 'single Gaussian' parametrization[12]; (3) a new 'multiple Gaussian' parametrization based on the experimental MM data.

4.1. Key findings

4.1.1. Improved characterization of edited MM signals—The first key finding was that experimental MM and multi-Gaussian approaches significantly reduced fit residuals compared to our previously devised single-Gaussian approach. The edited MM spectrum features three prominent signals: $MM_{0.94}$, $MM_{2.05}$, and $MM_{3.0}$. The co-edited $MM_{3.0}$ signal in the difference spectrum arises due to coupling to spins at 1.7 ppm, tentatively assigned to lysine- and arginine-containing compounds[13,30,51,52]. Similarly, the $MM_{0.94}$ signal is co-edited as a result of coupling to spins at 2 ppm, assigned to branched-chain amino acids, e.g. valine, leucine, and isoleucine[13,30,51,52]. The inverted resonance, $MM_{2.05}$, contains several contributing signals between 1.7 and 2.25 ppm, assigned to Glu/Gln-containing MMs. These are—like the tNAA methyl singlets—directly suppressed by the editing pulse during the edit-ON acquisition.

All observed MM signals in the difference spectrum exhibit an asymmetry that is insufficiently captured by single-Gaussian models such as the ones we have used to parametrize $MM_{0.94}$ and $MM_{3.0}$ (with a fixed amplitude ratio of 3:2) in our previous work[12]. This asymmetry likely arises because amino acids in MMs are arranged in three-dimensional chains, resulting in slightly different sets of chemical shifts (and, potentially, coupling constants) that depend on the protein structure and amino acid chain sequence. The distribution of chemical shifts is not necessarily normal or even symmetric[53]. Furthermore, the editing efficiency of a sinc-Gaussian editing pulse changes substantially over a range of ~10 Hz, meaning that some MMs will be edited with greater efficiency than others, even if their signal arises from the same amino acid.

Generally, different MRS analysis software packages vary greatly in the way that MM signals are treated in *J*-difference edited spectra[11]. Gannet[54] and Tarquin[55,56] include single- and double-Gaussian parameterizations of the composite GABA+ peak, respectively, without attempting to model GABA and $MM_{3.0}$ separately. The 'mega-press-3' setting of LCModel[57] defaults to a basis set that only includes GABA[58] and the spline baseline, but no explicit $MM_{3.0}$ term, although it includes an $MM_{0.94}$ signal.

While we previously investigated suitable parametrizations for $MM_{0.94}$ and $MM_{3.0}$[12], the addition of $MM_{2.05}$ is a new feature of this work, which further improved fit quality. We did explore sparser multiple-Gaussian parametrizations that only included subsets of the three peaks ($MM_{0.94}$, $MM_{3.0}$, and $MM_{2.05}$) but we found that fit residuals and baseline stability

were not as good (Supplementary Analysis 1). This suggested a stabilizing benefit of $MM_{0.94}$ and $MM_{2.05}$ as "anchor" signals for the MM model. Another suspected drawback of the fuller parameterization was the potential presence of unpredictable lipid signals, which might overlap with $MM_{0.94}$ and artifactually impact MM model contributions. We tested MM basis functions of varying sparsity in the presence of lipid signals (Supplementary Analysis 2) which included synthetic in-vivo-like lipid spectra (Supplementary Figures S6–S9) and actual lipid-contaminated in-vivo spectra (Supplementary Figures S10–S12). We found that utilizing the full parameterization was not detrimental to GABA+ estimation. In fact, the more complex MM representations exhibited better accuracy than sparse ones, whose GABA+ estimates were biased by the presence of lipids.

4.1.2. GABA/GABA+ ratio—The second key finding was that the relative contribution of co-edited $MM_{3.0}$ to GABA+ was estimated to be significantly larger by the experimental and multi-Gaussian approaches ($MM_{3.0}$/GABA+ = 58% on average) compared to the single-Gaussian approach (50% on average). $MM_{3.0}$/GABA+ values obtained with the new methods are at the upper end of previous estimates, which ranged between 41 and 60%, although only very few studies have explicitly attempted to quantify this ratio. Like us, several studies used inversion recovery to directly measure metabolite-nulled difference spectra. Three of these studies[22–24] then directly subtracted the subject-level metabolite-nulled edited MMs from the individual metabolite spectra; however, only one study provided an estimate for $MM_{3.0}$/GABA+ (41–49%)[23]. Rothman et al. directly compared integrals of $MM_{3.0}$ and GABA+ and estimated the ratio to be 60%, although at $2.1T^3$. A few applied studies described including metabolite-nulled MM spectra in their basis sets[26,27], but implementation details are scant and did not determine the relative contributions of $MM_{3.0}$ and GABA to GABA+. A second set of relevant references compared GABA estimates from MM-suppressed acquisitions to GABA+ estimates from MM-unsuppressed MEGA-PRESS and MEGA-SPECIAL, estimating $MM_{3.0}$/GABA+ integral ratios between 51–53%[59,60]. Finally, one study explored LCModel parametrizations of co-edited MMs that improved fit quality but did not report direct effects on the estimated relative GABA or MM fractions[25].

Our findings provide evidence that the GABA contribution to the GABA+ signal might be somewhat lower than the 50/50 ratio that is often referred to. This would have implications for the interpretation of MEGA-PRESS studies and observed changes in GABA+. We point out that peer-reviewed estimates of the GABA/GABA+ ratio are only provided in the second set of studies that compared MM-suppressed to MM-unsuppressed data. Crucially, these studies rest on the premise that the symmetric 'Henry'[6] editing scheme (with editing pulses at 1.9 and 1.5 ppm) reliably removes *all* co-edited MM to yield a 'pure' GABA signal. However, this assumption has come under scrutiny. First, Terpstra et al. estimated that the contribution of $MM_{3.0}$ to GABA+ can be as high as 15% in an (allegedly) MM-suppressed symmetric MEGA-sLASER experiment at $7T$[61]. It has since been demonstrated that lysine, the model metabolite for the $MM_{3.0}$ signal, is *not* perfectly nulled with the Henry editing scheme[41] (as shown in Figure 5 in the respective reference). Even if lysine *were* perfectly nulled, in-vivo MMs are not adequately approximated by lysine in solution, since, as discussed above, they will have a much broader set of chemical shifts and couplings. Symmetric editing has exactly one symmetry point where the two editing pulses have

the exact same inversion efficiency; therefore, it cannot possibly be perfectly symmetric with respect to *all* relevant MM spin systems. Lastly, it has been unequivocally shown that symmetric editing is at least an order of magnitude more susceptible to experimental instability[8,9] such as thermal frequency drift. It is unknown whether drift was sufficiently well-controlled in the studies that compared MM-suppressed GABA to MM-unsuppressed GABA+, and the 'purity' of the MM-suppressed GABA signal is therefore questionable. Assuming that the remaining signal—even after symmetric suppression—is *not* pure GABA, but GABA+ with some fraction of MM, the contribution of GABA to the overall GABA+ peak in the non-symmetric spectrum must be smaller than the often reported 50%.

4.2. Experimental considerations and limitations

There is some experimental evidence that $MM_{0.94}$ and $MM_{3.0}$ have different T_1[13], although it is far from conclusive. One study estimated T_1 at 463–518 ms for $MM_{3.0}$ and 280–284 ms for $MM_{0.94}$ in human brain at 9.4T[32]; another calculated 400 ms for $MM_{3.0}$ and 290 ms for $MM_{0.94}$ at 3T, although the 400-ms estimate appears to reach a pre-defined optimization boundary[62]. In contrast, another study of the rat brain at ultra-high field (17.2T)[63] found T_1 values of 748 ms for $MM_{0.94}$ and 574 ms for $MM_{3.0}$. If substantial T_1 differences were present, the use of a 'rigid' experimentally derived MM basis function may be inadequate, since it was acquired with a different T_1 weighting than the metabolite spectra that are being fit. The $MM_{0.94}$ and $MM_{3.0}$ components might therefore require appropriate individual scaling. In fact, if $T_1(MM_{3.0})$ were indeed longer than $T_1(MM_{0.94})$, the $MM_{3.0}$/ $MM_{0.94}$ area ratio in an up-scaled basis function would be smaller, and therefore likely absorb a smaller fraction of the composite GABA+ peak, since the $MM_{0.94}$ serves as a constraining 'modeling anchor'. However, while not implausible, we did not attempt such a correction while generating our basis functions because the current literature does not provide sufficiently robust evidence at 3T, and any correction we make may therefore be just as likely to introduce error rather than to correct.

In the pilot IR series we used to determine optimal TI, metabolite signals were found to be minimized at 650 ms at TR = 2000 ms. This choice of nulling TI is consistent with previous work[21,64]; similar work presented in conference proceedings used TI/TR = 525/1500 ms[23] and 580/1800 ms[22]. Even if a particular metabolite is perfectly nulled at a certain TI, the differences in T_1 between metabolites will inevitably lead to small residual signals in the nulled spectrum. Thankfully, in the case of *J*-difference-edited MMs, metabolites unperturbed by the editing pulse (e.g., tCr) are subtracted out during the generation of the difference spectrum. Contributions from major co-edited coupled metabolites (NAA and Glu) were identified in the edit-ON and edit-OFF spectra independently using an LCM approach with a reduced basis set.

We did not attempt to separate GABA from HCar, a dipeptide of GABA and histidine. HCar is present at considerable concentration in the human brain, but the spin system is so similar to GABA that it is virtually indistinguishable (~0.05 ppm chemical shift difference) at 3T. Due to this uncertainty, a large range of HCar concentration estimates have been reported in the literature (17–50% of the GABA concentration)[48,65,66]. Our previous attempts to

investigate the impact of including HCar in the LCM basis set suggested that it was indeed not separable from GABA[12].

While our results demonstrate the modeling benefits of experimentally acquired MM profiles, these results are presumed to be region- and sequence-specific. The relative contributions of GABA and MM to GABA+ will be strongly influenced by the field strength, TE, and the frequency/bandwidth of the editing pulses[67]. The editing pulse bandwidth, in particular, is an under-reported parameter in the literature and needs to be precisely matched in the experimental MM measurement. RF waveforms and timings can also influence the resulting signals, although, for the comparably broad MM profiles, we anticipate that these confounds will be less influential. A supplementary analysis of test-retest data acquired on a Siemens scanner[68] demonstrated improved within-subject CVs for GABA+ estimates using our experimental MM profiles compared to the single-Gaussian parameterization, despite the test-retest data being acquired using a different scanner vendor (Supplementary analysis 3). However, further study is required, and caution should be used when applying these experimental profiles beyond the conditions under which they were acquired. Furthermore, MM concentrations have been shown to be significantly higher in grey matter than white matter[69–71], indicating the regional dependence of MMs. Lastly, the sample size for our experimentally acquired edited MM basis function was relatively small and hampered by lipid contamination in some participants.

Conclusion

We present an improved characterization of GABA-edited difference spectra by using experimentally acquired MMs. Our mean MM basis function—and a new multiple-Gaussian parameterization method derived from it—reduced the amplitude and standard deviation of fit residuals compared to the previous single-Gaussian parameterization but suggested a larger relative contribution of the MMs to the GABA+ signal than commonly reported.

Supplementary Material

Refer to Web version on PubMed Central for supplementary material.

Funding

This work was supported by NIH grants R00 AG062230, R21 EB033516, R01 EB016089, R01 EB023963, P41 EB031771, S10 OD021648, K99 AG080084.

Data availability statement

- We have made the experimental MM basis function accessible—along with the code used to generate the analyses of this study—in an OSF repository (DOI: 10.17605/OSF.IO/QD37B)
- The BigGABA data are openly available in a NITRC repository (https://www.nitrc.org/projects/biggaba/)

References

1. Choi IY, Andronesi OC, Barker P, et al. Spectral editing in 1H magnetic resonance spectroscopy: Experts' consensus recommendations. NMR Biomed. 2021;34(5):e4411. doi:10.1002/nbm.4411 [PubMed: 32946145]
2. Mescher M, Merkle H, Kirsch J, Garwood M, Gruetter R. Simultaneous in vivo spectral editing and water suppression. NMR Biomed. 1998;11(6):266–272. doi:10.1002/(SICI)1099-1492(199810)11:6<266::AID-NBM530>3.0.CO;2-J [PubMed: 9802468]
3. Rothman DL, Petroff OA, Behar KL, Mattson RH. Localized 1H NMR measurements of gamma-aminobutyric acid in human brain in vivo. Proc Natl Acad Sci. 1993;90(12):5662–5666. doi:10.1073/pnas.90.12.5662 [PubMed: 8516315]
4. Mullins PG, McGonigle DJ, O'Gorman RL, et al. Current practice in the use of MEGA-PRESS spectroscopy for the detection of GABA. NeuroImage. 2014;86:43–52. doi:10.1016/j.neuroimage.2012.12.004 [PubMed: 23246994]
5. Peek AL, Rebbeck TJ, Leaver AM, et al. A comprehensive guide to MEGA-PRESS for GABA measurement. Anal Biochem. 2023;669:115113. doi:10.1016/j.ab.2023.115113 [PubMed: 36958511]
6. Henry PG, Dautry C, Hantraye P, Bloch G. Brain GABA editing without macromolecule contamination. Magn Reson Med. 2001;45(3):517–520. doi:10.1002/1522-2594(200103)45:3<517::AID-MRM1068>3.0.CO;2-6 [PubMed: 11241712]
7. Edden RAE, Puts NAJ, Barker PB. Macromolecule-suppressed GABA-edited magnetic resonance spectroscopy at 3T. Magn Reson Med. 2012;68(3):657–661. doi:10.1002/mrm.24391 [PubMed: 22777748]
8. Edden RAE, Oeltzschner G, Harris AD, et al. Prospective frequency correction for macromolecule-suppressed GABA editing at 3T. J Magn Reson Imaging. 2016;44(6):1474–1482. doi:10.1002/jmri.25304 [PubMed: 27239903]
9. Harris AD, Glaubitz B, Near J, et al. Impact of frequency drift on gamma-aminobutyric acid-edited MR spectroscopy. Magn Reson Med. 2014;72(4):941–948. doi:10.1002/mrm.25009 [PubMed: 24407931]
10. Andronesi OC, Bhattacharyya PK, Bogner W, et al. Motion correction methods for MRS: experts' consensus recommendations. NMR Biomed. 2021;34(5):e4364. doi:10.1002/nbm.4364 [PubMed: 33089547]
11. Craven AR, Bhattacharyya PK, Clarke WT, et al. Comparison of seven modelling algorithms for γ-aminobutyric acid–edited proton magnetic resonance spectroscopy. NMR Biomed. 2022;35(7):e4702. doi:10.1002/nbm.4702 [PubMed: 35078266]
12. Zöllner HJ, Tapper S, Hui SCN, Barker PB, Edden RAE, Oeltzschner G. Comparison of linear combination modeling strategies for edited magnetic resonance spectroscopy at 3 T. NMR Biomed. 2022;35(1):e4618. doi:10.1002/nbm.4618 [PubMed: 34558129]
13. Cudalbu C, Behar KL, Bhattacharyya PK, et al. Contribution of macromolecules to brain 1H MR spectra: Experts' consensus recommendations. NMR Biomed. 2021;34(5):e4393. doi:10.1002/nbm.4393 [PubMed: 33236818]
14. Hofmann L, Slotboom J, Jung B, Maloca P, Boesch C, Kreis R. Quantitative 1H-magnetic resonance spectroscopy of human brain: Influence of composition and parameterization of the basis set in linear combination model-fitting. Magn Reson Med. 2002;48(3):440–453. doi:10.1002/mrm.10246 [PubMed: 12210908]
15. Pfeuffer J, Tkáč I, Provencher SW, Gruetter R. Toward an in Vivo Neurochemical Profile: Quantification of 18 Metabolites in Short-Echo-Time 1H NMR Spectra of the Rat Brain. J Magn Reson. 1999;141(1):104–120. doi:10.1006/jmre.1999.1895 [PubMed: 10527748]
16. Cudalbu C, Mlynárik V, Xin L, Gruetter R. Quantification of in vivo short echo-time proton magnetic resonance spectra at 14.1 T using two different approaches of modelling the macromolecule spectrum. Meas Sci Technol. 2009;20(10):104034. doi:10.1088/0957-0233/20/10/104034

17. Giapitzakis IA, Borbath T, Murali-Manohar S, Avdievich N, Henning A. Investigation of the influence of macromolecules and spline baseline in the fitting model of human brain spectra at 9.4T. Magn Reson Med. 2019;81(2):746–758. doi:10.1002/mrm.27467 [PubMed: 30329186]
18. Schaller B, Xin L, Cudalbu C, Gruetter R. Quantification of the neurochemical profile using simulated macromolecule resonances at 3 T. NMR Biomed. 2013;26(5):593–599. doi:10.1002/nbm.2896 [PubMed: 23413241]
19. Birch R, Peet AC, Dehghani H, Wilson M. Influence of macromolecule baseline on 1H MR spectroscopic imaging reproducibility. Magn Reson Med. 2017;77(1):34–43. doi:10.1002/mrm.26103 [PubMed: 26800478]
20. Zöllner HJ, Davies-Jenkins CW, Murali-Manohar S, et al. Feasibility and implications of using subject-specific macromolecular spectra to model short echo time magnetic resonance spectroscopy data. NMR Biomed. 2023;36(3):e4854. doi:10.1002/nbm.4854 [PubMed: 36271899]
21. Hui SCN, Gong T, Zöllner HJ, et al. The macromolecular MR spectrum does not change with healthy aging. Magn Reson Med. 2022;87(4):1711–1719. doi:10.1002/mrm.29093 [PubMed: 34841564]
22. O'Gorman RL, Edden RAE, Michels L, Murdoch JB, Martin E. Precision and repeatability of in vivo GABA and glutamate quantification. In: 19th Annual Meeting of the International Society for Magnetic Resonance in Medicine (ISMRM). ; 2011. https://archive.ismrm.org/2011/3434.html. Accessed August 22, 2023.
23. Kegeles LS, Mao X, Gonsalez R, Shungu DC. Evaluation of Anatomic Variation in Macromolecule Contribution to the GABA Signal Using Metabolite Nulling and the J-Editing Technique at 3.0 T. In: 15th Annual Meeting of the International Society for Magnetic Resonance in Medicine (ISMRM).
24. Stagg CJ, Wylezinska M, Matthews PM, et al. Neurochemical Effects of Theta Burst Stimulation as Assessed by Magnetic Resonance Spectroscopy. J Neurophysiol. 2009;101(6):2872–2877. doi:10.1152/jn.91060.2008 [PubMed: 19339458]
25. Murdoch JB, Dydak U. Modeling MEGA-PRESS Macromolecules for a Better Grasp of GABA. In: 19th Annual Meeting of the International Society for Magnetic Resonance in Medicine (ISMRM). ; 2011. https://archive.ismrm.org/2011/1394.html. Accessed August 22, 2023.
26. Duncan NW, Wiebking C, Tiret B, et al. Glutamate Concentration in the Medial Prefrontal Cortex Predicts Resting-State Cortical-Subcortical Functional Connectivity in Humans. PLOS ONE. 2013;8(4):e60312. doi:10.1371/journal.pone.0060312 [PubMed: 23573246]
27. Tremblay S, Beaulé V, Proulx S, et al. Relationship between transcranial magnetic stimulation measures of intracortical inhibition and spectroscopy measures of GABA and glutamate+glutamine. J Neurophysiol. 2013;109(5):1343–1349. doi:10.1152/jn.00704.2012 [PubMed: 23221412]
28. Mikkelsen M, Barker PB, Bhattacharyya PK, et al. Big GABA: Edited MR spectroscopy at 24 research sites. NeuroImage. 2017;159:32–45. doi:10.1016/j.neuroimage.2017.07.021 [PubMed: 28716717]
29. High magnetic field water and metabolite proton T1 and T2 relaxation in rat brain in vivo - de Graaf - 2006 - Magnetic Resonance in Medicine - Wiley Online Library. https://onlinelibrary.wiley.com/doi/full/10.1002/mrm.20946. Accessed July 21, 2023.
30. Behar KL, Ogino T. Assignment of resonances in the 1H spectrum of rat brain by two-dimensional shift correlated and j-resolved NMR spectroscopy. Magn Reson Med. 1991;17(2):285–303. doi:10.1002/mrm.1910170202 [PubMed: 1676483]
31. Cudalbu C, Mlynárik V, Xin L, Gruetter R. Comparison of T1 relaxation times of the neurochemical profile in rat brain at 9.4 tesla and 14.1 tesla. Magn Reson Med. 2009;62(4):862–867. doi:10.1002/mrm.22022 [PubMed: 19645007]
32. Murali-Manohar S, Wright AM, Borbath T, Avdievich NI, Henning A. A novel method to measure T1-relaxation times of macromolecules and quantification of the macromolecular resonances. Magn Reson Med. 2021;85(2):601–614. doi:10.1002/mrm.28484 [PubMed: 32864826]
33. Puts NAJ, Barker PB, Edden RAE. Measuring the longitudinal relaxation time of GABA in vivo at 3 tesla. J Magn Reson Imaging. 2013;37(4):999–1003. doi:10.1002/jmri.23817 [PubMed: 23001644]

34. Lin A, Andronesi O, Bogner W, et al. Minimum Reporting Standards for in vivo Magnetic Resonance Spectroscopy (MRSinMRS): Experts' consensus recommendations. NMR Biomed. 2021;34(5):e4484. doi:10.1002/nbm.4484 [PubMed: 33559967]
35. Oeltzschner G, Zöllner HJ, Hui SCN, et al. Osprey: Open-source processing, reconstruction & estimation of magnetic resonance spectroscopy data. J Neurosci Methods. 2020;343:108827. doi:10.1016/j.jneumeth.2020.108827 [PubMed: 32603810]
36. Wilson M, Andronesi O, Barker PB, et al. Methodological consensus on clinical proton MRS of the brain: Review and recommendations. Magn Reson Med. 2019;82(2):527–550. doi:10.1002/mrm.27742 [PubMed: 30919510]
37. Near J, Harris AD, Juchem C, et al. Preprocessing, analysis and quantification in single-voxel magnetic resonance spectroscopy: experts' consensus recommendations. NMR Biomed. 2021;34(5):e4257. doi:10.1002/nbm.4257 [PubMed: 32084297]
38. Klose U In vivo proton spectroscopy in presence of eddy currents. Magn Reson Med. 1990;14(1):26–30. doi:10.1002/mrm.1910140104 [PubMed: 2161984]
39. Mikkelsen M, Tapper S, Near J, Mostofsky SH, Puts NAJ, Edden RAE. Correcting frequency and phase offsets in MRS data using robust spectral registration. NMR Biomed. 2020;33(10):e4368. doi:10.1002/nbm.4368 [PubMed: 32656879]
40. Lin L, Považan M, Berrington A, Chen Z, Barker PB. Water removal in MR spectroscopic imaging with L2 regularization. Magn Reson Med. 2019;82(4):1278–1287. doi:10.1002/mrm.27824 [PubMed: 31148254]
41. Deelchand DK, Marjańska M, Henry PG, Terpstra M. MEGA-PRESS of GABA+: Influences of acquisition parameters. NMR Biomed. 2021;34(5):e4199. doi:10.1002/nbm.4199 [PubMed: 31658398]
42. Vanhamme L, van den Boogaart A, Van Huffel S. Improved Method for Accurate and Efficient Quantification of MRS Data with Use of Prior Knowledge. J Magn Reson. 1997;129(1):35–43. doi:10.1006/jmre.1997.1244 [PubMed: 9405214]
43. Simicic D, Rackayova V, Xin L, et al. In vivo macromolecule signals in rat brain 1H-MR spectra at 9.4T: Parametrization, spline baseline estimation, and T2 relaxation times. Magn Reson Med. 2021;86(5):2384–2401. doi:10.1002/mrm.28910 [PubMed: 34268821]
44. RStudio Team. RStudio: Integrated Development Environment for R. Boston, MA; 2020. http://www.rstudio.com/.
45. Zöllner HJ, Považan M, Hui SCN, Tapper S, Edden RAE, Oeltzschner G. Comparison of different linear-combination modeling algorithms for short-TE proton spectra. NMR Biomed. 2021;34(4):e4482. doi:10.1002/nbm.4482 [PubMed: 33530131]
46. Marjańska M, Terpstra M. Influence of fitting approaches in LCModel on MRS quantification focusing on age-specific macromolecules and the spline baseline. NMR Biomed. 2021;34(5):e4197. doi:10.1002/nbm.4197 [PubMed: 31782845]
47. Marjańska M, Deelchand DK, Kreis R, Team the 2016 IMSGFC. Results and interpretation of a fitting challenge for MR spectroscopy set up by the MRS study group of ISMRM. Magn Reson Med. 2022;87(1):11–32. doi:10.1002/mrm.28942 [PubMed: 34337767]
48. Govindaraju V, Young K, Maudsley AA. Proton NMR chemical shifts and coupling constants for brain metabolites. NMR Biomed. 2000;13(3):129–153. doi:10.1002/1099-1492(200005)13:3<129::AID-NBM619>3.0.CO;2-V [PubMed: 10861994]
49. Hui SCN, Saleh MG, Zöllner HJ, et al. MRSCloud: A cloud-based MRS tool for basis set simulation. Magn Reson Med. 2022;88(5):1994–2004. doi:10.1002/mrm.29370 [PubMed: 35775808]
50. Simpson R, Devenyi GA, Jezzard P, Hennessy TJ, Near J. Advanced processing and simulation of MRS data using the FID appliance (FID-A)—An open source, MATLAB-based toolkit. Magn Reson Med. 2017;77(1):23–33. doi:10.1002/mrm.26091 [PubMed: 26715192]
51. Behar KL, Rothman DL, Spencer DD, Petroff OAC. Analysis of macromolecule resonances in 1H NMR spectra of human brain. Magn Reson Med. 1994;32(3):294–302. doi:10.1002/mrm.1910320304 [PubMed: 7984061]
52. Behar KL, Ogino T. Characterization of macromolecule resonances in the 1H NMR spectrum of rat brain. Magn Reson Med. 1993;30(1):38–44. doi:10.1002/mrm.1910300107 [PubMed: 8371672]

53. Borbath T, Murali-Manohar S, Henning A. Towards a Fitting Model of Macromolecular Spectra: Amino Acids. In: 27th Annual Meeting of the International Society for Magnetic Resonance in Medicine (ISMRM). ; 2019. https://cds.ismrm.org/protected/19MProceedings/PDFfiles/1068.html. Accessed August 28, 2023.
54. Edden RAE, Puts NAJ, Harris AD, Barker PB, Evans CJ. Gannet: A batch-processing tool for the quantitative analysis of gamma-aminobutyric acid–edited MR spectroscopy spectra. J Magn Reson Imaging. 2014;40(6):1445–1452. doi:10.1002/jmri.24478 [PubMed: 25548816]
55. Wilson M, Reynolds G, Kauppinen RA, Arvanitis TN, Peet AC. A constrained least-squares approach to the automated quantitation of in vivo 1H magnetic resonance spectroscopy data. Magn Reson Med. 2011;65(1):1–12. doi:10.1002/mrm.22579 [PubMed: 20878762]
56. Reynolds G, Wilson M, Peet A, Arvanitis TN. An algorithm for the automated quantitation of metabolites in in vitro NMR signals. Magn Reson Med. 2006;56(6):1211–1219. doi:10.1002/mrm.21081 [PubMed: 17029227]
57. Provencher SW. Estimation of metabolite concentrations from localized in vivo proton NMR spectra. Magn Reson Med. 1993;30(6):672–679. doi:10.1002/mrm.1910300604 [PubMed: 8139448]
58. Provencher SW. Automatic quantitation of localized in vivo 1H spectra with LCModel. NMR Biomed. 2001;14(4):260–264. doi:10.1002/nbm.698 [PubMed: 11410943]
59. Near J, Simpson R, Cowen P, Jezzard P. Efficient γ-aminobutyric acid editing at 3T without macromolecule contamination: MEGA-SPECIAL. NMR Biomed. 2011;24(10):1277–1285. doi:10.1002/nbm.1688 [PubMed: 21387450]
60. Harris AD, Puts NAJ, Barker PB, Edden RAE. Spectral-editing measurements of GABA in the human brain with and without macromolecule suppression. Magn Reson Med. 2015;74(6):1523–1529. doi:10.1002/mrm.25549 [PubMed: 25521836]
61. Terpstra M, Ugurbil K, Gruetter R. Direct in vivo measurement of human cerebral GABA concentration using MEGA-editing at 7 Tesla. Magn Reson Med. 2002;47(5):1009–1012. doi:10.1002/mrm.10146 [PubMed: 11979581]
62. Hoefemann M, Bolliger CS, Chong DGQ, van der Veen JW, Kreis R. Parameterization of metabolite and macromolecule contributions in interrelated MR spectra of human brain using multidimensional modeling. NMR Biomed. 2020;33(9):e4328. doi:10.1002/nbm.4328 [PubMed: 32542861]
63. Lopez-Kolkovsky AL, Mériaux S, Boumezbeur F. Metabolite and macromolecule T1 and T2 relaxation times in the rat brain in vivo at 17.2T. Magn Reson Med. 2016;75(2):503–514. doi:10.1002/mrm.25602 [PubMed: 25820200]
64. Bhattacharyya PK, Phillips MD, Stone LA, Bermel RA, Lowe MJ. Sensorimotor Cortex Gamma-Aminobutyric Acid Concentration Correlates with Impaired Performance in Patients with MS. Am J Neuroradiol. 2013;34(9):1733–1739. doi:10.3174/ajnr.A3483 [PubMed: 23493890]
65. Petroff OAC, Mattson RH, Behar KL, Hyder F, Rothman DL. Vigabatrin increases human brain homocarnosine and improves seizure control. Ann Neurol. 1998;44(6):948–952. doi:10.1002/ana.410440614 [PubMed: 9851440]
66. Landheer K, Prinsen H, Petroff OA, Rothman DL, Juchem C. Elevated homocarnosine and GABA in subject on isoniazid as assessed through 1H MRS at 7T. Anal Biochem. 2020;599:113738. doi:10.1016/j.ab.2020.113738 [PubMed: 32302606]
67. Harris AD, Puts NAJ, Wijtenburg SA, et al. Normalizing data from GABA-edited MEGA-PRESS implementations at 3 Tesla. Magn Reson Imaging. 2017;42:8–15. doi:10.1016/j.mri.2017.04.013 [PubMed: 28479342]
68. Hupfeld KE, Zöllner HJ, Hui SCN, et al. Impact of acquisition and modeling parameters on the test–retest reproducibility of edited GABA+. NMR Biomed. n/a(n/a):e5076. doi:10.1002/nbm.5076
69. Považan M, Hangel G, Strasser B, et al. Mapping of brain macromolecules and their use for spectral processing of 1H-MRSI data with an ultra-short acquisition delay at 7T. NeuroImage. 2015;121:126–135. doi:10.1016/j.neuroimage.2015.07.042 [PubMed: 26210813]

70. Schaller B, Xin L, Gruetter R. Is the macromolecule signal tissue-specific in healthy human brain? A 1H MRS study at 7 tesla in the occipital lobe. Magn Reson Med. 2014;72(4):934–940. doi:10.1002/mrm.24995 [PubMed: 24407736]

71. Hofmann L, Slotboom J, Boesch C, Kreis R. Characterization of the macromolecule baseline in localized 1H-MR spectra of human brain. Magn Reson Med. 2001;46(5):855–863. doi:10.1002/mrm.1269 [PubMed: 11675635]

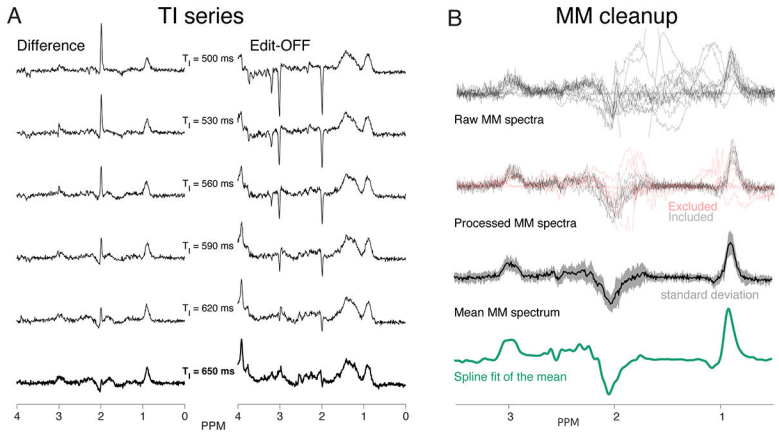

Figure 1.

(A) An example of the full TI series from a single subject. The left panel shows the difference spectrum, while the right panel shows the edit-OFF spectrum. TI = 650 ms was selected as optimal, as it minimized the contributions of the metabolites. (B) The stages of MM processing. From top-to-bottom: the individual subject-level raw MM spectra, the individual subject-level processed MM spectra after ‘clean-up’ (rejected subjects in red), the mean MM spectrum across subjects (black) with the standard deviation across the included MMs (light shaded area), and the spline fit of the mean MM spectrum (green).

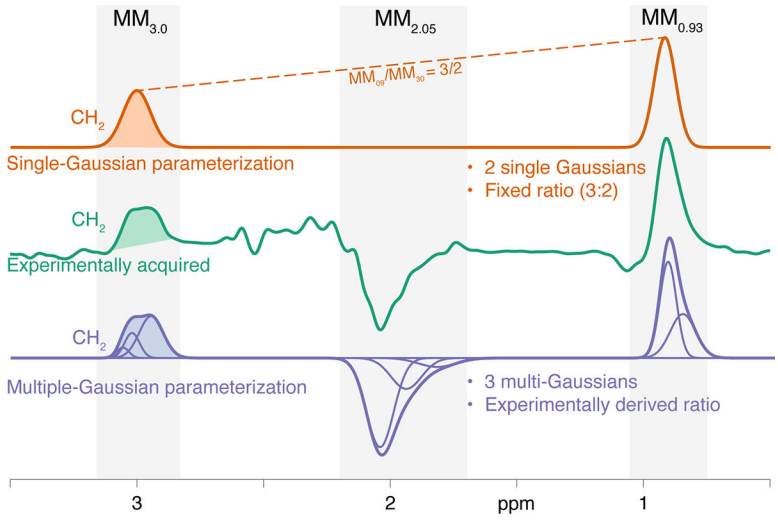

Figure 2.

The three composite MM basis functions used in our comparative analysis (solid lines) and the areas used to reference them to a CH_2 group. From top-to-bottom: our previously published "best practice" parameterization of the MMs[12], comprised of two single-Gaussian functions to represent the $MM_{0.94}$ and $MM_{3.0}$ signals with a fixed amplitude ratio (orange); the experimentally acquired MM basis function derived from the TI = 650 ms dataset (green); and the new multiple-Gaussian parameterization, with the sum (bold purple line) of the individual Gaussians (fine purple lines) used as a single basis function.

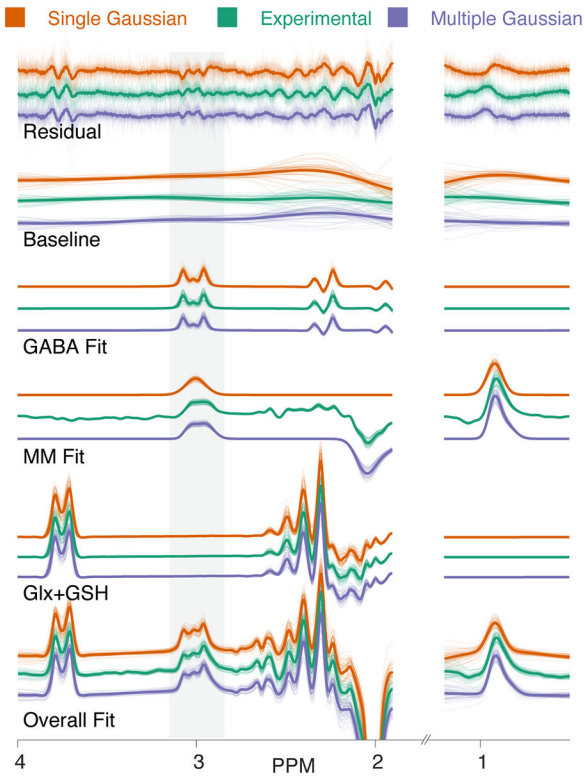

Figure 3.

The individual (fine lines) and mean (bold lines) LCM results are shown. From the top to the bottom: fit residual, spline baseline, GABA fits, MM fits, (Glu + Gln + GSH) fits, and overall fit are shown for the single-Gaussian parametrization we previously published (orange), the experimental MM (green), and the new multi-Gaussian parametrization (purple).

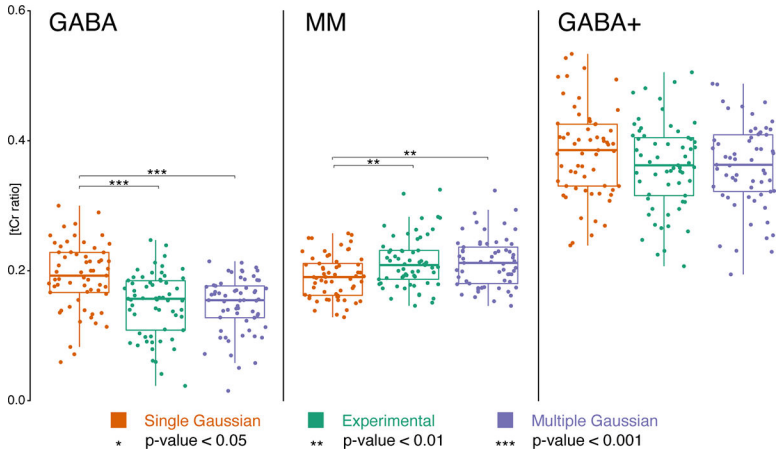

Figure 4.

Boxplots for fitted amplitudes resolved by MM handling procedure: single-Gaussian parametrization previously published (orange), experimental MM (green), and new multi-Gaussian parametrization (purple). From left to right, boxplots show the reported ratios-to-tCr for GABA, MM, and GABA+. Significant differences between the analyses are identified using paired t-tests and marked with an increasing number of asterisks for *p*-values < 0.05, 0.01, and 0.001, respectively.

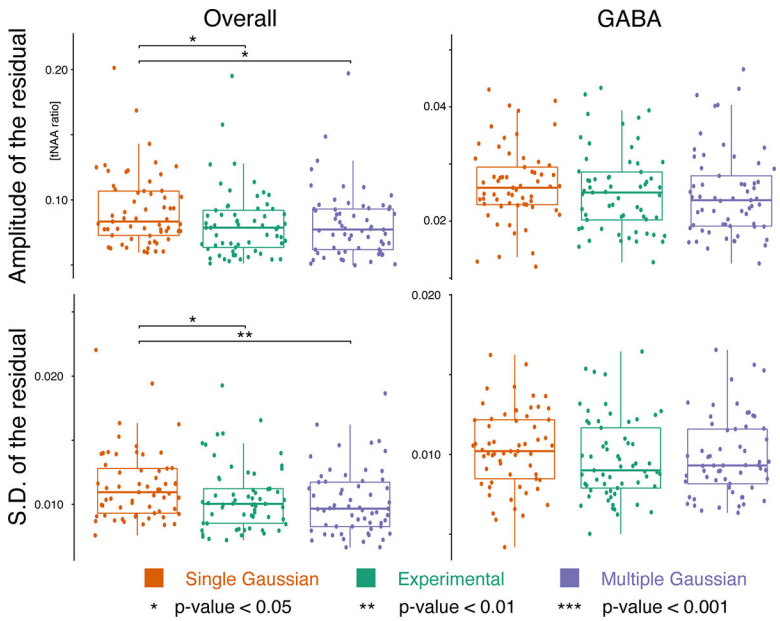

Figure 5.

Boxplots for fitting metrics resolved by MM handling procedure: single-Gaussian parametrization previously published (orange), experimental MM (green), and new multi-Gaussian parametrization (purple). Boxplots show the amplitude of the residual (top row) and standard deviation of the residual (bottom row) across the full fit range (left column) and for the frequency range around GABA at 3 ppm (right column), all normalized to total NAA. Significant differences between the analyses are identified using paired t-tests and marked with an increasing number of asterisks for p-values < 0.05, 0.01, and 0.001, respectively.

Table 1.

Gaussian parameterization of the experimental MM profile as derived from AMARES. The columns are the peak group fitted, center frequencies of the Gaussian functions (ppm), amplitude of the individual Gaussian functions, and the linewidth of the Gaussian functions (FWHM, Hz).

Peak group	Frequency [ppm]	Amplitude	Phase	linewidth [Hz]
$MM_{0.93}$	0.86	1.34	0	15.00
$MM_{0.93}$	0.92	1.90	0	9.70
$MM_{2.05}$	1.82	0.40	180	22.00
$MM_{2.05}$	1.95	1.13	180	18.00
$MM_{2.05}$	2.05	2.90	180	16.00
$MM_{3.0}$	2.95	1.20	0	14.10
$MM_{3.0}$	3.02	0.45	0	8.84
$MM_{3.0}$	3.06	0.15	0	7.06